Characterization of Human Keratinocyte Cell Lines for Barrier Studies

Mary C. Moran[1,2,3], Radha P. Pandya[2,3], Kimberly A. Leffler[2], Takeshi Yoshida[2], Lisa A. Beck[2] and Matthew G. Brewer[2]

Epidermal cell models are critical for studying skin biology. The gold standard used by the scientific community has historically been primary cell cultures from discarded tissue, typically from neonates (foreskin). Although directly applicable to humans, this system suffers from multiple issues, including substantial donor-to-donor variability and a finite number of divisions in culture. As such, we have identified a faithful alternative called N/TERT2G cells. These cells show many of the characteristics of primary cells, including barrier formation, differentiation kinetics and/or protein expression, and pathogenesis. From our observations, N/TERT2G cells can serve as a reproducible and genetically manipulatable platform in studying skin biology.

JID Innovations (2021);**1:**100018 doi:10.1016/j.xjidi.2021.100018

INTRODUCTION

The epidermis protects the body from pathogens, allergens, irritants, and pollutants and limits water loss. Keratinocytes (KCs), the main epidermal cell, undergo differentiation to form four distinct layers: stratum basale, stratum spinosum, stratum granulosum, and stratum corneum (SC). The physical barrier of the epidermis is maintained by two structures. The first is in the SC and consists of corneocytes surrounded by a complex lipid matrix, and underneath this in the stratum granulosum where cell-cell junctions called tight junctions (TJs), are found.

Studies of the human epidermis have relied on primary cells propagated as monolayers or bilayers or three-dimensional organotypic raft cultures. Our laboratory and many others have shown that differentiated primary KCs form TJs in vitro, but they have multiple limitations, such as their finite number of cell divisions. In addition, their supply is not reliable, and there is a considerable variation in biological assays, which may be a function of donor variation (e.g., anatomic location, health, sex, and age). This highlights the need for a cell line that faithfully recapitulates primary KCs with regard to cellular differentiation, barrier formation, and TJ organization. Identification of such an alternative would also provide an opportunity to genetically manipulate key proteins to address their biological relevance.

To address this, we compared the key features of three KC types: primary human foreskin KCs (PHFKs), N/TERT2G cells (immortalized PHFK, human telomerase, and spontaneous mutation), and HaCaT cells (spontaneously immortalized KCs) (Boukamp et al., 1988; Dickson et al., 2000). Previous studies have independently compared HaCaT or N/TERT cells with primary KCs, focusing on differentiation and SC formation (Seo et al., 2012; Smits et al., 2017; van Drongelen et al., 2014). They found that N/TERT cells grown as a human epidermal equivalent model are comparable with primary human KCs, with similar SC organization, SC permeability, and differentiation marker expression (Smits et al., 2017; van Drongelen et al., 2014). HaCaT cells showed dissimilar responses to cytokine stimulation compared with primary KC in the expression of cornified envelope transcripts, suggesting that HaCaT cells are not a suitable alternative to primary KC (Seo et al., 2012). We extended these findings by comparing these KC cell lines focusing on differentiation markers (at the protein level), immunoreactivity of TJ proteins, physiological barrier function, and viral infectivity using in vitro monolayer models. We show that N/TERT2G cells recapitulate PHFKs in differentiation, TJ organization, formation of a functional barrier, and susceptibility to viral infections.

RESULTS AND DISCUSSION

We first compared barrier function, measured by transepithelial electrical resistance (TEER), in these different KC models. PHFKs developed increased TEER (i.e., greater barrier function) after differentiation was initiated by exposure to high calcium media (1.8 mM) (Boston BioProducts, Ashland, MA) (Figure 1a) (Bikle et al., 2012). Using the same differentiation media, N/TERT2G cells also demonstrated increased TEER over time after the initiation of differentiation; however, TEER was statistically less in N/TERT2G cells at three time points (Figure 1a). N/TERT2G cells reached peak TEER earlier than PHFKs, in agreement with a previous study showing that N/TERT2G cells differentiate more rapidly than primary KCs (Smits et al., 2017). In contrast, HaCaT cells did not form a robust barrier, as demonstrated by no increase in

[1]*Department of Microbiology & Immunology, University of Rochester Medical Center, Rochester, New York, USA; and* [2]*Department of Dermatology, University of Rochester Medical Center, Rochester, New York, USA*

[3]*These authors contributed equally to this work.*

Correspondence: Matthew G. Brewer, Department of Dermatology, University of Rochester Medical Center, 601 Elmwood Avenue, Rochester, New York 14642, USA. E-mail: matthew_brewer@urmc.rochester.edu

Abbreviations: CK, cytokeratin; KC, keratinocyte; PHFK, primary human foreskin keratinocyte; SC, stratum corneum; TEER, transepithelial electrical resistance; TJ, tight junction

Received 16 December 2020; revised 30 March 2021; accepted 31 March 2021; accepted manuscript published online 28 April 2021; corrected proof published online 29 May 2021

Cite this article as: JID Innovations 2021;1:100018

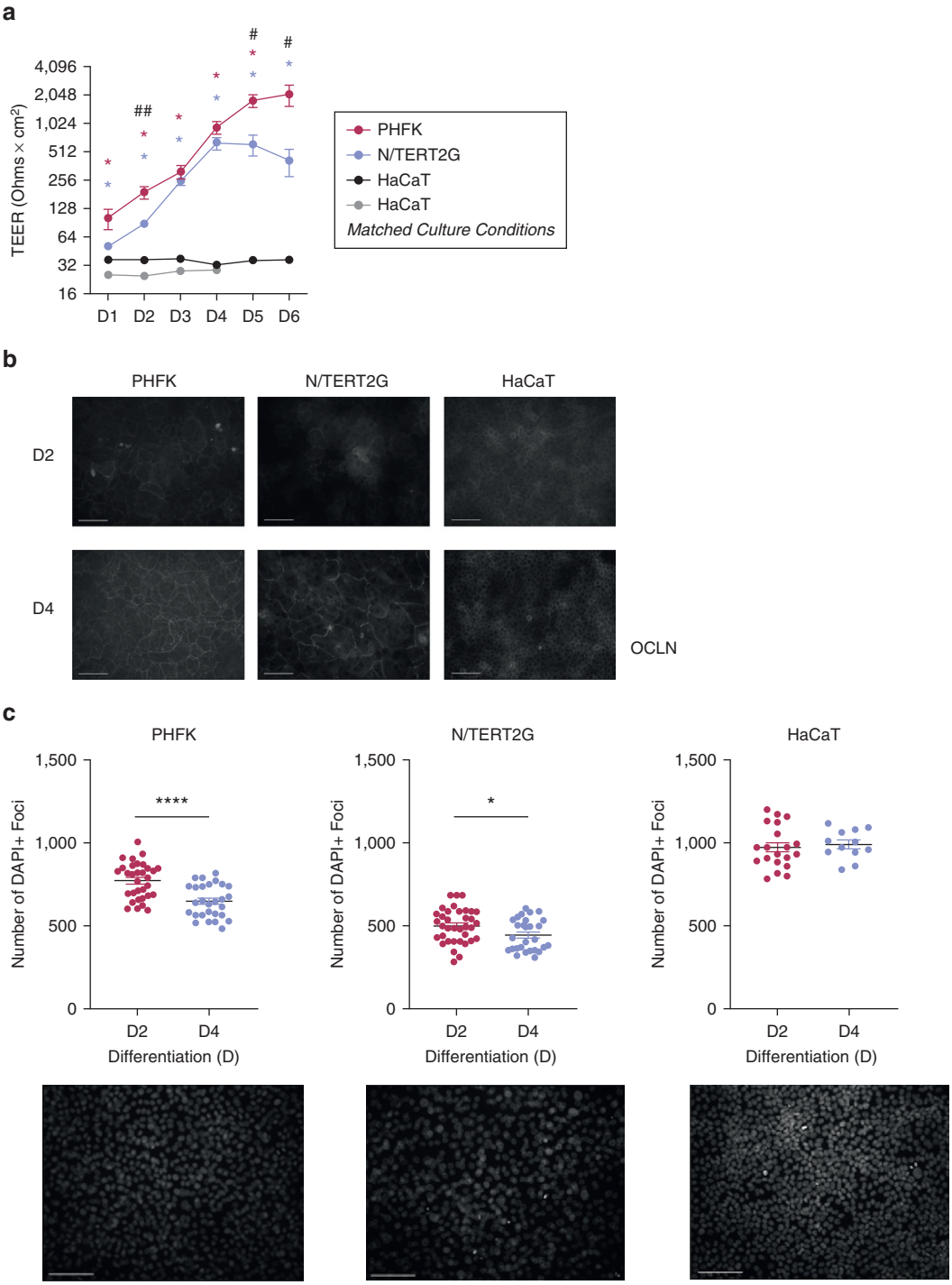

Figure 1. PHFKs and N/TERT2G cells form barriers and display similar OCLN immunoreactivity during differentiation. Cells were grown to confluence and switched to media containing calcium (1.8 mM) to initiate differentiation (PHFK-, N/TERT2G-, HaCaT-matched culture conditions), HaCaT cells were grown in recommended media (DMEM + 10% fetal bovine serum and penicillin, streptomycin, and amphotericin additives). (**a**) TEER was measured for 6 Ds after differentiation (n = 5 PHFKs and N/TERT2G cells, n = 3 HaCaT cells). Mann–Whitney *U* test comparing PHFKs versus HaCaT cells (*), N/TERT2G cells versus HaCaT cells (*), and PHFKs versus N/TERT2G cells (#) at each time point. (**b**) Immunofluorescence staining for OCLN at D2 and D4 after differentiation. Images were captured at an exposure time of 850 ms (for PHFKs and N/TERT2G cells) or 3,000 ms (for HaCaT cells). (**c**) Four images from each slide (1−2 slides) of each donor or passage at D2 and D4 were quantified for the number of $DAPI^+$ cells per image. n = 4 PHFKs, n = 3 N/TERT2G cells, n = 3 HaCaT cells. Representative images were taken on D2. Bar =100 μm. $^{\#}P < 0.05$, $^{*}P < 0.05$, $^{\#\#}P < 0.01$, $^{****}P < 0.0001$. Shown is the mean ± SEM of the data. D, day; ms, millisecond; PHFK, primary human foreskin keratinocyte; TEER, transepithelial electrical resistance.

TEER values (Figure 1a). This is despite the fact that they do appear to differentiate as noted by an increase in the differentiation marker, cytokeratin (CK)-10 (Figure 2a). To ensure that this barrier abnormality was not due to different culture conditions, we cultured HaCaT cells in the media conditions used for PHFKs and N/TERT2G cells. HaCaT cells were

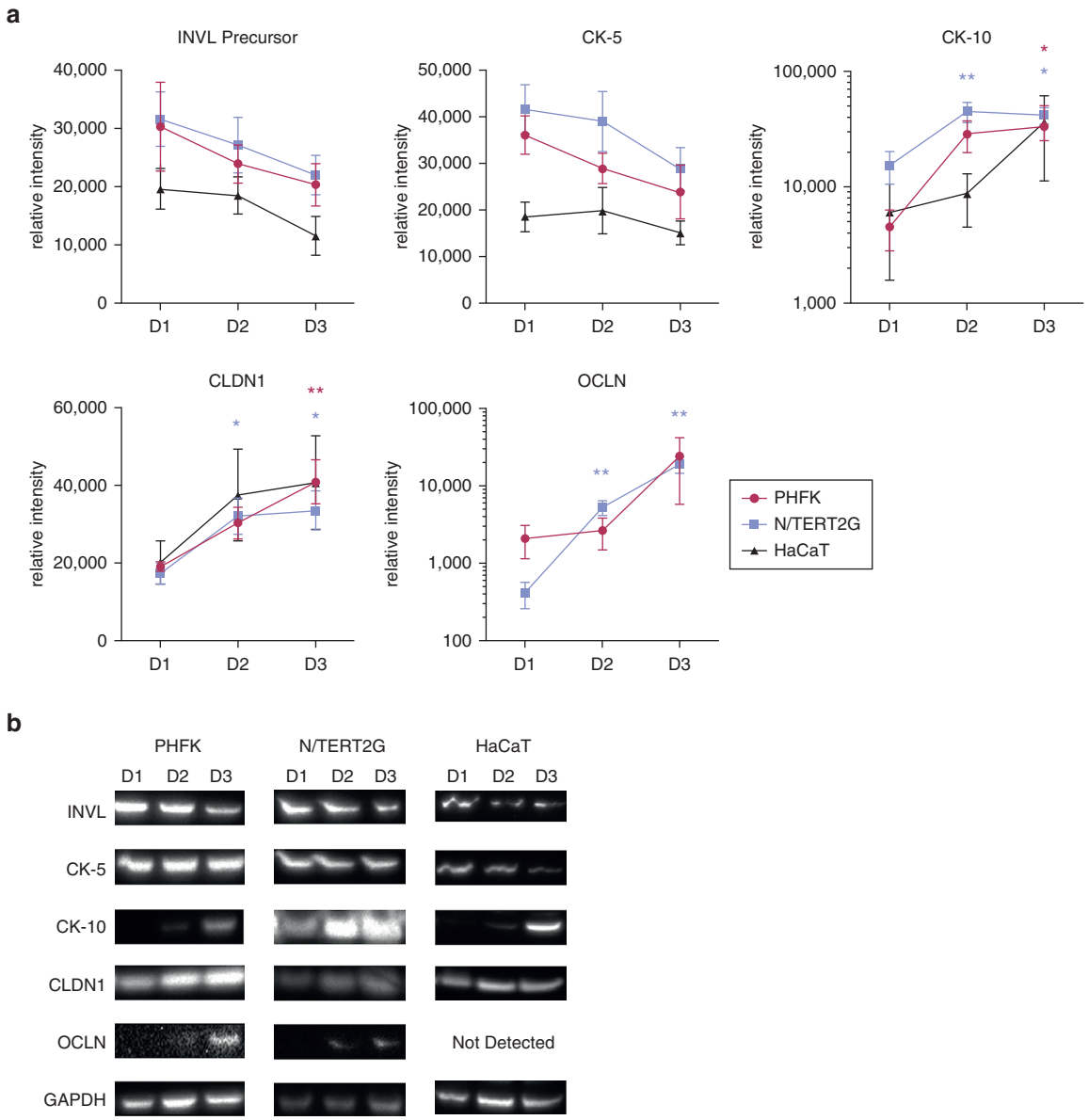

Figure 2. PHFKs, N/TERT2G cells, and HaCaT cells have approximately similar expression patterns of epidermal differentiation markers and TJ barrier proteins. (**a**) Cell lysates were collected on D1, D2, and D3 after differentiation, and INVL precursor, CK-5 and CK-10, and TJ proteins CLDN1 and OCLN were detected by western blot analysis. OCLN was not detected in HaCaT cells. Expression was quantified by densitometry with normalization to GAPDH expression. (**b**) Representative blots. Molecular weight (kDa) approximation by ladder: 68 for INVL precursor, 58 for CK-5, 60 for CK-10, 23 for CLDN-1, 59 for OCLN, and 37 for GAPDH. (n = 4–7 PHFKs; n = 5–8 N/TERT2G cells; n = 3–6 HaCaT cells). Shown is the mean ± SEM of the data. Mann–Whitney *U* test comparing D1 with D2 and D1 with D3 within each cell type. $*P < 0.05$, $**P < 0.01$. CK, cytokeratin; CLDN1, claudin-1; D, day; INVL, involucrin; OCLN, occludin; PHFK, primary human foreskin keratinocyte; TJ, tight junction.

cultured in KC serum–free media (Invitrogen, Carlsbad, CA), and at confluency, they were exposed to the media used to induce differentiation in PHFKs and N/TERT2G cells (DMEM with 1.8 mM calcium ion) (Thermo Fisher Scientific, Waltham, MA). HaCaT cells did not develop barrier formation as measured by TEER using these culturing conditions either, suggesting that barrier formation as a result of high calcium exposure is not possible in these cells (Figure 1a).

The movement of TJ transmembrane proteins to the cell–cell borders is a critical step in the formation of a robust barrier. Immunofluorescence staining for the TJ transmembrane proteins, OCLN and CLDN1, was performed on PHFKs, N/TERT2G cells, and HaCaT cells. OCLN was the first TJ protein identified, and it plays an important role in barrier function for most epithelia (Saitou et al., 2000). Reductions in CLDN1 have been observed in patients with atopic dermatitis, and *Cldn1*-knockout mice die shortly after birth owing to cutaneous water loss, implicating its importance in barrier function (De Benedetto et al., 2011a, 2011b; Furuse et al., 2002). Two days after differentiation, all the three cell types display circumferential OCLN immunoreactivity and the formation of the characteristic honeycomb pattern (Brewer et al., 2020). The only KC cell line that showed distinct circumferential staining for OCLN at day 2 after differentiation was PHFK; yet, this pattern was still somewhat incomplete and was not seen across the entire field (Figure 1b). By day 4 after differentiation,

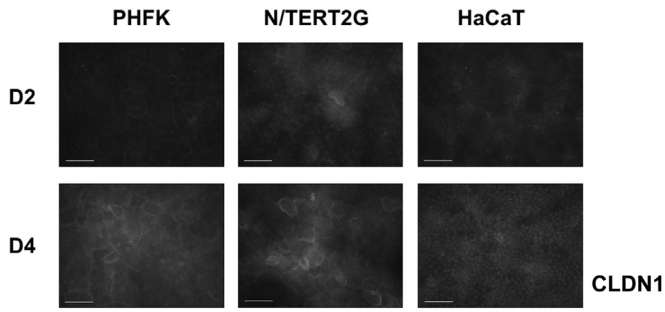

Figure 3. PHFKs and N/TERT2G cells demonstrate similar CLDN1 reorganization during differentiation. Immunofluorescent staining of the TJ protein CLDN1 on D2 and D4 after differentiation. Representative images were taken at each time point. Images were captured with an exposure time of 850 ms (for PHFKs and N/TERT2G cells) or 3,000 ms (for HaCaT cells). Bar = 100 μm. D, day; ms, millisecond; PHFK, primary human foreskin keratinocyte; TJ, tight junction.

the honeycomb pattern was very defined and observed throughout the field in PHFKs. N/TERT2G cells demonstrated clear circumferential OCLN immunoreactivity at day 4 after differentiation, but this was less evenly distributed than that demonstrated by PHFKs. This suggests that the localization of OCLN to the cell–cell borders is delayed in N/TERT2G cells compared with that in PHFKs, which may explain their lower TEER level. HaCaT cells showed minimal OCLN immunoreactivity, as demonstrated by its significantly longer exposure time (3.5-fold longer) and diffuse localization (Figure 1b).

PHFKs and N/TERT2G cells also showed similar reorganization of CLDN1 during differentiation (Figure 3). On day 2 after differentiation, CLDN1 was localized in the nucleus, with some cytoplasmic and circumferential localization. On day 4 after differentiation, the circumferential localization of CLDN1 in PHFKs and N/TERT2G cells was more distinct. CLDN1 immunoreactivity remained localized to the nucleus in HaCaT cells at both time points. CLDN1 contains a nuclear localization sequence, and its localization to the nucleus has been previously reported (Hagen, 2017). Finally, using the nuclear stain, DAPI, we observed that HaCaT cells were both smaller and more densely packed than either PHFKs or N/TERT2G cells (Figure 1c). This is consistent with the smaller and more tightly packed pattern of OCLN we observed in HaCaT cells (Figure 1b). Importantly, HaCaT cells grow much faster than either PHFKs or N/TERT2G cells, most likely owing to their cancer-derived nature (Boukamp et al., 1988). Together, this supports the conclusion that both PHFKs and N/TERT2G cells form distinct, honeycomb-like TJ structures, albeit with slightly delayed kinetics in N/TERT2G cells. In contrast, HaCaT cells do not have immunoreactivity for key TJ transmembrane proteins at their cell surface even after 4 days of confluency.

The sharp, circumferential outline of OCLN and CLDN1 immunoreactivity observed in the PHFK images may in part explain the higher TEER measurements. On day 2 after differentiation, we observed the most significant difference in TEER between PHFKs and N/TERT2G cells (Figure 1a). This coincides with a more disorganized TJ protein localization in N/TERT2G cells than in PHFKs (Figure 1b). On day 4 after differentiation, whereas OCLN organization was still not as defined in N/TERT2G cells as in PHFKs, the proteins were beginning to localize to the cell–cell borders (Figure 1b). This coincides with continued increases in TEER and with a time point (day 4) in differentiation when TEER is no longer significantly different between N/TERT2G cells and PHFKs (Figure 1a).

We next compared the expression patterns of key differentiation markers by western blot. Expression of CK-5 (expressed in the stratum basale) and CK-10 and involucrin precursor (both expressed in the stratum spinosum) were quantified on days 1, 2, and 3 after differentiation (Leung et al., 2020). We observed similar expression patterns of these differentiation markers, with CK-10 expression increasing, and slight decreases in CK-5 and involucrin precursor as differentiation progressed (Figure 2a and b). HaCaT cells demonstrated similar but less consistent expression patterns than PHFKs and N/TERT2G cells. Protein expression of the TJ proteins, CLDN1 and OCLN, increased over time in PHFKs and N/TERT2G cells, aligning with TEER formation (Figures 1a and 2a). OCLN was not detected in HaCaT cells by western blot, which is consistent with our observation that the immunofluorescent staining required substantially higher exposure times to visualize immunoreactivity (Figures 1b and 2a). This differs from the findings of a previous study in which OCLN was detected in HaCaT cells by western blot (Aono and Hirai, 2008). It is important to note that the OCLN antibodies used in the assay in this study were polyclonal (Zymed Laboratories, South San Francisco, CA) whereas ours was monoclonal and from a different manufacturer (Invitrogen). In addition, the media used to culture their HaCaT cells had a substantially higher concentration of calcium (9.8 mM) than those used by most investigators (1.8 mM) in the field of epidermal biology (Bikle et al., 2012; Goleva et al., 2019; Howell et al., 2008), which could explain the confounding observations. Furthermore, it was acknowledged that culturing of HaCaT cells with the traditional calcium concentration of 1.8 mM did not allow for the formation of TJs (Aono and Hirai, 2008). As noted earlier, this may explain the lack of TEER in HaCaT cells (Figure 1a). Interestingly, HaCaT cells expressed CLDN1 (predominantly in the nucleus), despite the fact that they did not form a robust barrier as measured by TEER. This disparity suggests that these cells may have an abnormality in the trafficking of TJ-associated transmembrane proteins to the cell surface, which was suggested by our immunofluorescent staining (Figures 1b and 3).

Our laboratory has had a longstanding interest in understanding why patients with atopic dermatitis have enhanced susceptibility to cutaneous pathogens (Beck et al., 2009; De Benedetto et al., 2011b). The skin microbiota of patients with atopic dermatitis is dominated by *Staphylococcus aureus* colonization, and skin colonization strongly correlates with disease severity and barrier disruption (Kong et al., 2012; Simpson et al., 2018; Tauber et al., 2016). We therefore evaluated TEER changes in response to stimulation with *S. aureus* supernatants. We found that PHFKs and N/TERT2G cells responded similarly to supernatants from USA300, a highly virulent strain of community-associated methicillin-resistant *S. aureus*. Specifically, we observed a significant reduction in TEER, providing further evidence that N/TERT2G cells respond similarly to PHFKs (Figure 4). We noted that the TEER reduction after USA300 treatment in N/TERT2G cells

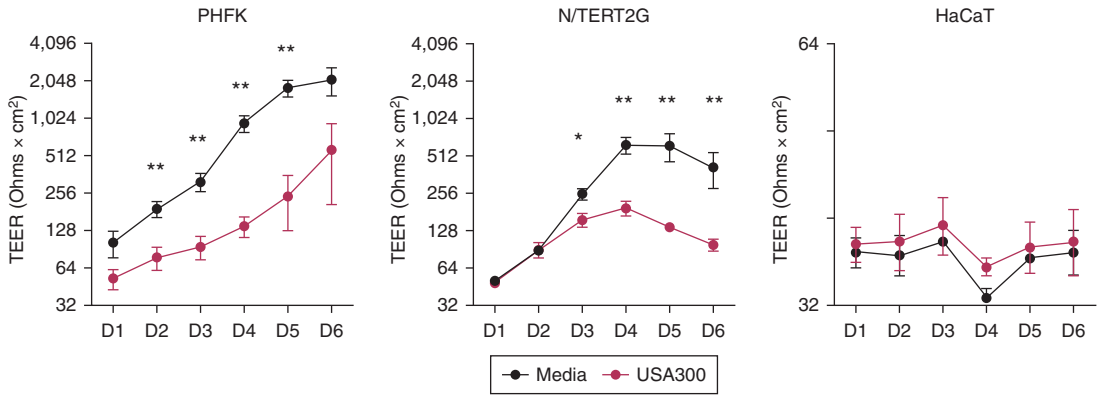

Figure 4. Treatment with *Staphylococcus aureus* supernatants significantly decreases barrier function in PHFKs and N/TERT2G cells. Cells were grown to confluence and switched to media containing calcium (1.8 mM) to initiate differentiation (PHFKs, N/TERT2G cells); HaCaT cells were grown in recommended media. TEER was measured in cells with and without exposure to *S. aureus* supernatant at 15 μg/ml (n = 5 PHFKs and N/TERT2G cells; n = 3 HaCaT cells). Mann–Whitney *U* test. **P* < 0.05, ***P* < 0.01. Shown is the mean ± SEM of the data. D, day; PHFK, primary human foreskin keratinocyte; TEER, transepithelial electrical resistance.

was a bit delayed compared with that in PHFKs. We speculate that this is a result of the low TEER values observed from N/TERT2G cells early during differentiation, which makes it difficult to detect changes in TEER after the USA300 treatment. PHFKs form a robust barrier following differentiation, making it easier to detect TEER changes in response to treatments. Characterizing the effects and understanding the mechanisms of *S. aureus* supernatants on TJ organization and differentiation are the focus of ongoing studies.

It has been shown that changes in barrier function can alter susceptibility to viral infection and that disrupted epidermal barrier and altered KC differentiation are often observed together (De Benedetto et al., 2011b; Guttman-Yassky et al., 2009; Schleimer and Berdnikovs, 2017). We tested whether PHFKs and N/TERT2G cells have similar susceptibility to vaccinia virus infection at different stages of differentiation. We chose vaccinia virus because it is a viral pathogen that uniquely affects patients with atopic dermatitis, leading to severe viremia and causing a life-threatening condition called eczema vaccinatum. We observed similar patterns of susceptibility, whereby undifferentiated and PHFKs and N/TERT2G cells infected on day 2 after differentiation were less permissive to vaccinia virus infection. Both PHFKs and N/TERT2G cells were highly susceptible to vaccinia virus infection when cells were infected at the time of initiating differentiation by exposure to calcium-containing media (Figure 5). These data suggest that PHFKs and N/TERT2G cells become highly susceptible to infection with vaccinia virus within the first 24 hours of differentiation, since cells were exposed to the virus during that time period of the differentiation process. We hypothesize that the increased susceptibility to viral infection observed when KCs are infected at the time of differentiation is a result of the remarkable changes in gene expression that occur when differentiation is induced in KCs (Toufighi et al., 2015). Understanding how differentiation influences susceptibility to infection is also the focus of the ongoing research.

In summary, we have shown that N/TERT2G cells faithfully recapitulate primary human KCs. This immortalized cell line circumvents the limitations of PHFKs, such as donor variability, limited cell divisions, and poor scalability. It is important to note that most laboratories working with

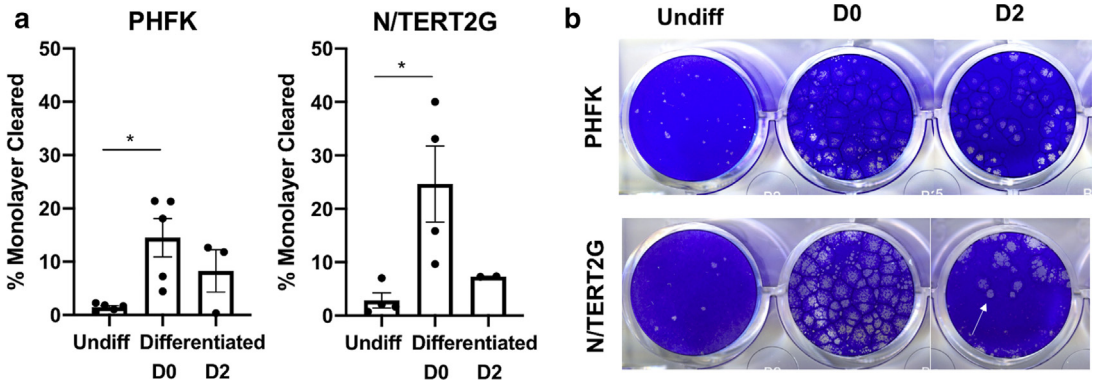

Figure 5. State of differentiation determines susceptibility to viral infection in PHFKs and N/TERT2G cells. Cells were infected with a low MOI (0.0001) of vaccinia virus while Undiff, at the time of differentiation (D0), or 2 days after differentiation (D2). Plates were stained with crystal violet 48 hours after infection to visualize plaque formation (arrow). (**a**) ImageJ was used to calculate the percentage of the monolayer within each well that was cleared by plaques. (**b**) Representative images of crystal violet plates and plaques. n = 5 PHFKs; n = 4 N/TERT2G cells. Significance was calculated using the Kruskal–Wallis test, **P* < 0.05. Shown is the mean ± SEM of the data. D, day; MOI, multiplicity of infection; PHFK, primary human foreskin keratinocyte; Undiff, undifferentiated.

primary cells acknowledge that many PHFK preparations do not propagate well and therefore cannot be used for in vitro experiments. In our hands, ~30% of isolated KCs do not propagate or develop barrier function (i.e., elevations in TEER) and therefore cannot be used in experiments. This identifies the need for alternative KC models that provide a more robust and reproducible epidermal model. Finally, an immortalized cell line such as N/TERT2G provides the opportunity to genetically manipulate the expression of key proteins using techniques such as CRISPR/Cas9 as we have recently shown with the knock down of *CLDN1* and *CD40* (unpublished data). The studies presented in this paper support N/TERT2G cells as a suitable alternative to PHFKs for numerous assays important to skin biology.

Table 1. Antibodies Used for Western Blot Analysis

Antibodies	Manufacturer	Dilution
Anti-CLDN1 (519000)	Invitrogen	1:1,000
Anti-GAPDH (0411) HRP	Santa Cruz Biotechnology	1:5,000
Anti-cytokeratin 5 (EP1601)	Abcam	1:5,000
Anti-keratin 10 (Poly 19054)	BioLegend	1:1,000
Anti-involucrin (Poly 19244)	BioLegend	1:1,000
Anti-occludin (OC3F10)	Invitrogen	1:500
Anti-mouse IgG HRP (NA931V)	Sigma-Aldrich	1:5,000
Anti-rabbit IgG HRP (NA934V)	Sigma-Aldrich	1:5,000

Abbreviation: HRP, horseradish peroxidase.

MATERIALS AND METHODS

Cell cultures

PHFKs were isolated from discarded human neonatal foreskin tissue. Patient consent for experiments was not required because human tissue left over from surgery was deidentified and was considered discarded material. The use of deidentified and discarded human skin tissues for research use was approved by the Research Subject Review Board at the University of Rochester Medical Center (Rochester, NY) (URMC IRB STUDY: 00004672). Isolation and propagation procedures for PHFKs were done as previously described (Poumay and Pittelkow, 1995; Poumay et al., 1994). N/TERT2G cells were provided by Ellen H. van den Bogaard and grown as previously described (Dickson et al., 2000; Smits et al., 2017). HaCaT cells were grown in DMEM containing 10% fetal bovine serum and penicillin, streptomycin, and amphotericin additives. PHFKs and N/TERT2G cells were switched to DMEM media supplemented with 1.8 mM calcium ion and 4 mM glutamine (Thermo Fisher Scientific) to induce differentiation. Days after differentiation referred to the number of days since exposure to the supplemented DMEM. For HaCaT cells, in which there was no media switch to induce differentiation, days after differentiation referred to the number of days since cells became confluent.

S. aureus culturing

The *S. aureus* strain USA300 (FRP3757) was grown, and supernatants were filtered as previously described (Moran et al., 2019). Protein content was determined using the Pierce BCA Protein Assay Kit (Thermo Fisher Scientific).

TEER

TEER measurements were done as previously published (De Benedetto et al., 2011b). Measurements of TEER were taken for up to 6 days after the initiation of differentiation and exposure to USA300 supernatant.

Immunofluorescent staining of TJ formation in PHFKs, N/TERT2G cells, and HaCaT cells

PHFKs, N/TERT2G cells, and HaCaT cells were plated onto sterilized glass coverslips and stained for immunofluorescent analysis for OCLN, CLDN1, and DAPI as previously described (Brewer et al., 2020).

Immunofluorescent imaging of OCLN, CLDN1, and DAPI staining using fluorescent microscopy

PHFK, N/TERT2G, and HaCaT slides were imaged using SPOT RT3 (Diagnostic Instruments, Sterling Heights, MI) on an Olympus BX60 fluorescent microscope, and ImageJ software was used to analyze the images. All DAPI-stained images were acquired at 100 milliseconds exposure. OCLN and CLDN images were acquired at 850 milliseconds exposure for PHFKs and N/TERT cells. OCLN and CLDN images of HaCaT cells were acquired at 3,000 milliseconds exposure. Four DAPI-stained images were captured from each donor or cell passage on day 2 and day 4 after differentiation. Quantification of $DAPI^+$ foci per image was accomplished in ImageJ using the threshold function to remove background noise and to convert the image to black and white. After this, the watershed tool was used to outline individual cells. The analyze particles function was used to quantify nuclei-sized pixels using a pixel range of 500 to infinity, which was chosen to exclude the pixels too small to be nuclei. Each data point represents the number of $DAPI^+$ foci in each image of $n = 4$ PHFKs, $n = 3$ N/TERT2G cells, and $n = 3$ HaCaT cells (1−2 slides per donor or passage, four images per slide).

Western blot analysis

PHFKs, N/TERT2G cells, and HaCaT cells were grown to confluency. Differentiation was induced in PHFKs and N/TERT2G cells (DMEM + 1.8 mM calcium ion + 4 mM glutamine), whereas HaCaT cells remained in standard culture media. Cell lysates (RIPA buffer [Boston BioProducts] containing protease and phosphatase inhibitors [Sigma-Aldrich, St. Louis, MO] with 0.2% SDS [Thermo Fisher Scientific]) were collected on days 1, 2, and 3 after differentiation. Samples were run on Invitrogen NuPAGE 4−12% Bis-Tris gels and transferred to polyvinylidene fluoride membrane (Bio-Rad Laboratories, Hercules, CA). Membranes were probed with the antibodies shown in Table 1. Antibodies were detected using SuperSignal West Pico PLUS Chemiluminescent Substrate (Thermo Fisher Scientific). Relative protein expression was determined by densitometry calculated using ImageJ software. Samples were normalized to GAPDH expression and protein content (Pierce BCA Protein Assay Kit).

Vaccinia virus infection assay

PHFKs and N/TERT2G cells were plated at a density of 150,000 cells per well in a 24-well plate. Cells were infected with a low multiplicity of infection of the Western Reserve strain of vaccinia virus (multiplicity of infection of 0.0001) while undifferentiated, at the time of differentiation, or 2 days after differentiation. Infection media were removed 24 hours after infection and replaced with fresh media. Crystal violet was added to the cells 48 hours after the initial infection. ImageJ software was used to calculate the percentage of the monolayer within each well that was cleared by plaques. To do this, each well was selected with the region of interest tool (circle), and the image was duplicated (right click, duplicate). The total area of the circle was determined by using Analyze -> Measure. Next, the outside of the circle was cleared using the Edit -> Clear Outside

command; then the threshold function was applied to the image so that the cleared monolayer (plaques) is white: Image -> Adjust -> Threshold -> Apply. Finally, all area considered to be plaques was selected using the Edit -> Selection -> Create Selection, and the selection was inverted using the Make Inverse function. The area covered by plaques was measured as described earlier (Analyze -> Measure), and the area covered in plaques was divided by the total area to get the percentage monolayer cleared.

Statistical analysis

Statistics were run using GraphPad Prism (GraphPad, San Diego, CA). Mann–Whitney *U* tests were used for analysis. Kruskal–Wallis test was used for Figure 5.

Data availability statement

No datasets were generated or analyzed during this study.

ORCIDs

Mary C. Moran http://orcid.org/0000-0002-6456-082X
Radha P. Pandya: http://orcid.org/0000-0002-3105-1666
Kimberly A. Leffler https://orcid.org/0000-0002-7633-8732
Takeshi Yoshida: http://orcid.org/0000-0003-0133-5067
Lisa A. Beck: http://orcid.org/0000-0002-8452-667X
Matthew G. Brewer: http://orcid.org/0000-0001-7631-5234

AUTHOR CONTRIBUTIONS

Conceptualization: MGB, LAB; Formal Analysis: MCM, RPP, KAL; Funding Acquisition: LAB, MGB; Investigation: MCM, RPP; Project Administration; MGB, LAB; Resources: TY; Supervision: MGB, LAB; Visualization: MCM, RPP; Writing - Original Draft Preparation: MCM, RPP; Writing - Review and Editing: MGB, LAB, TY

ACKNOWLEDGMENTS

We acknowledge Ellen H. van den Bogaard for providing the N/TERT2G cells. We would also like to acknowledge the Neonatology Division at the University of Rochester Medical Center (Rochester, NY) for providing primary human foreskin keratinocyte samples (URMC IRB STUDY: 00003986). MCM is partially supported by the National Institute of Allergy and Infectious Diseases (T32 AI118689). Additional supports by the National Institute of Allergy and Infectious Diseases (U01AI152011; to LAB and MGB) and Pfizer (58273087; to LAB and MGB) were provided.

CONFLICT OF INTEREST

LAB declares being a consultant for AbbVie, Allakos, AstraZeneca, BenevolentAI Bio, DermTech, Incyte, Janssen Pharmaceuticals, LEO Pharma, Eli Lilly, Novartis, Pfizer, Principia Biopharma, RAPT Therapeutics, Regeneron Pharmaceuticals, Sanofi/Genzyme, Sanofi-Aventis, and Stealth Biotherapeutics; declares being an investigator for AbbVie, LEO Pharma, Pfizer, Regeneron Pharmaceuticals, and Sanofi; and owns stock in Medtronic, 3M, Moderna, and Gilead Sciences.

The remaining authors state no conflict of interest.

REFERENCES

Aono S, Hirai Y. Phosphorylation of claudin-4 is required for tight junction formation in a human keratinocyte cell line. Exp Cell Res 2008;314:3326–39.

Beck LA, Boguniewicz M, Hata T, Schneider LC, Hanifin J, Gallo R, et al. Phenotype of atopic dermatitis subjects with a history of eczema herpeticum. J Allergy Clin Immunol 2009;124:260–9.e2697.

Bikle DD, Xie Z, Tu CL. Calcium regulation of keratinocyte differentiation. Expert Rev Endocrinol Metab 2012;7:461–72.

Boukamp P, Petrussevska RT, Breitkreutz D, Hornung J, Markham A, Fusenig NE. Normal keratinization in a spontaneously immortalized aneuploid human keratinocyte cell line. J Cell Biol 1988;106:761–71.

Brewer MG, Anderson EA, Pandya RP, De Benedetto A, Yoshida T, Hilimire TA, et al. Peptides derived from the tight junction protein CLDN1 disrupt the skin barrier and promote responsiveness to an epicutaneous vaccine. J Invest Dermatol 2020;140:361–9.e3.

De Benedetto A, Rafaels NM, McGirt LY, Ivanov AI, Georas SN, Cheadle C, et al. Tight junction defects in patients with atopic dermatitis. J Allergy Clin Immunol 2011a;127:773–86.e1–7.

De Benedetto A, Slifka MK, Rafaels NM, Kuo IH, Georas SN, Boguniewicz M, et al. Reductions in claudin-1 may enhance susceptibility to herpes simplex virus 1 infections in atopic dermatitis [published correction appears in J Allergy Clin Immunol 2011;128:903]. J Allergy Clin Immunol 2011b;128:242–6.e5.

Dickson MA, Hahn WC, Ino Y, Ronfard V, Wu JY, Weinberg RA, et al. Human keratinocytes that express hTERT and also bypass a p16(INK4a)-enforced mechanism that limits life span become immortal yet retain normal growth and differentiation characteristics. Mol Cell Biol 2000;20:1436–47.

Furuse M, Hata M, Furuse K, Yoshida Y, Haratake A, Sugitani Y, et al. Claudin-based tight junctions are crucial for the mammalian epidermal barrier: a lesson from claudin-1-deficient mice. J Cell Biol 2002;156:1099–111.

Goleva E, Berdyshev E, Leung DY. Epithelial barrier repair and prevention of allergy. J Clin Invest 2019;129:1463–74.

Guttman-Yassky E, Suárez-Fariñas M, Chiricozzi A, Nograles KE, Shemer A, Fuentes-Duculan J, et al. Broad defects in epidermal cornification in atopic dermatitis identified through genomic analysis. J Allergy Clin Immunol 2009;124:1235–44.e58.

Hagen SJ. Non-canonical functions of claudin proteins: beyond the regulation of cell-cell adhesions. Tissue Barriers 2017;5:e1327839.

Howell MD, Fairchild HR, Kim BE, Bin L, Boguniewicz M, Redzic JS, et al. Th2 cytokines act on S100/A11 to downregulate keratinocyte differentiation. J Invest Dermatol 2008;128:2248–58.

Kong HH, Oh J, Deming C, Conlan S, Grice EA, Beatson MA, et al. Temporal shifts in the skin microbiome associated with disease flares and treatment in children with atopic dermatitis. Genome Res 2012;22:850–9.

Leung DYM, Berdyshev E, Goleva E. Cutaneous barrier dysfunction in allergic diseases. J Allergy Clin Immunol 2020;145:1485–97.

Moran MC, Cahill MP, Brewer MG, Yoshida T, Knowlden S, Perez-Nazario N, et al. Staphylococcal virulence factors on the skin of atopic dermatitis patients. mSphere 2019;4:e00616–9.

Poumay Y, Roland IH, Leclercq-Smekens M, Leloup R. Basal detachment of the epidermis using dispase: tissue spatial organization and fate of integrin alpha 6 beta 4 and hemidesmosomes. J Invest Dermatol 1994;102:111–7.

Poumay Y, Pittelkow MR. Cell density and culture factors regulate keratinocyte commitment to differentiation and expression of suprabasal K1/K10 keratins. J Invest Dermatol 1995;104:271–6.

Saitou M, Furuse M, Sasaki H, Schulzke JD, Fromm M, Takano H, et al. Complex phenotype of mice lacking occludin, a component of tight junction strands. Mol Biol Cell 2000;11:4131–42.

Schleimer RP, Berdnikovs S. Etiology of epithelial barrier dysfunction in patients with type 2 inflammatory diseases. J Allergy Clin Immunol 2017;139:1752–61.

Seo MD, Kang TJ, Lee CH, Lee AY, Noh M. HaCaT keratinocytes and primary epidermal keratinocytes have different transcriptional profiles of cornified envelope-associated genes to T Helper cell cytokines. Biomol Ther (Seoul) 2012;20:171–6.

Simpson EL, Villarreal M, Jepson B, Rafaels N, David G, Hanifin J, et al. Patients with atopic dermatitis colonized with Staphylococcus aureus have a distinct phenotype and endotype. J Invest Dermatol 2018;138:2224–33.

Smits JPH, Niehues H, Rikken G, van Vlijmen-Willems I, van de Zande G, Zeeuwen P, et al. Immortalized N/TERT keratinocytes as an alternative cell source in 3D human epidermal models. Sci Rep 2017;7:11838.

Tauber M, Balica S, Hsu CY, Jean-Decoster C, Lauze C, Redoules D, et al. Staphylococcus aureus density on lesional and nonlesional skin is strongly associated with disease severity in atopic dermatitis. J Allergy Clin Immunol 2016;137:1272–4.e3.

Toufighi K, Yang JS, Luis NM, Aznar Benitah S, Lehner B, Serrano L, et al. Dissecting the calcium-induced differentiation of human primary keratinocytes stem cells by integrative and structural network analyses. PLoS Comput Biol 2015;11:e1004256.

van Drongelen V, Danso MO, Mulder A, Mieremet A, van Smeden J, Bouwstra JA, et al. Barrier properties of an N/TERT-based human skin equivalent. Tissue Eng Part A 2014;20:3041–9.